

Compounding and molding of polyethylene composites reinforced with keratin feather fiber[☆]

Justin R. Barone ^{*}, Walter F. Schmidt, Christina F.E. Liebner

USDA/ARS/ANRI/EQL, Bldg. 012, Rm. 1-3, BARC-West, 10300 Baltimore Ave., Beltsville, MD 20705, USA

Received 9 April 2004; received in revised form 22 September 2004; accepted 29 September 2004

Available online 10 December 2004

Abstract

Polyethylene-based composites are prepared using keratin feather fiber obtained from chicken feathers. Keratin fibers are mixed into high-density polyethylene (HDPE) at 20 wt% using a Brabender mixing head. This is the compounding step and the variables studied are compounding time, temperature, speed and state of fiber dispersion. Following compounding, the composites are compression molded at various times and temperatures and this is the molding step. The effects of compounding and molding are studied using tensile testing and scanning electron microscopy. It is found that keratin feather fiber provides a stiffness increase to HDPE but lowers tensile breaking stress. The fibers are thermally stable for long periods of time up to 200 °C, but the best composite properties are found at processing temperatures of 205 °C, where the fibers are only stable for a few minutes.

© 2004 Elsevier Ltd. All rights reserved.

Keywords: A. Fibres; A. Polymer–matrix composite (PMCs); A. Short-fiber composites; B. Mechanical properties; B. Microstructure

1. Introduction

There has been recent interest in developing composites based on short-fibers obtained from agricultural resources. These organic fibers are usually of lower density than inorganic fibers, environmentally friendly, and relatively easy to obtain. Although the absolute property increase when using organic fibers is not anticipated to be nearly as high as when using inorganic fibers, the specific properties are anticipated to be high owing to the much lower density of the organic fibers [1,2]. In addition, organic fibers have a slower rate of length reduction than inorganic fibers during melt extrusion [3]. This is important because the aspect, i.e., length to

diameter (L/D), ratio of the fiber is a factor in determining the final composite properties [4].

Most studies of naturally occurring organic fibers concentrate on cellulose-based fibers obtained from renewable plant resources such as China reed, wood, flax, sisal, or jute [5–14]. There are very few studies detailing composites made from protein fibers obtained from agricultural resources. Barone and Schmidt [15] recently reported on the use of keratin feather fiber as a short-fiber reinforcement in LDPE composites. The keratin feather fiber is obtained from the over four billion pounds of chicken feather waste generated by the U.S. poultry industry each year [16]. The structure and properties of the keratin feather fiber are described in detail elsewhere [15,17,18]. Poultry feather fiber is predominantly keratin protein in an α -helix structure with a crystalline melting point of about 240 °C [17,18]. There are many studies detailing the physical properties of whole bird feathers and the quill portion of the feather [19–22]. Reported modulus and strength values of whole

[☆] Mention of trade names or commercial products in this article is solely for the purpose of providing specific information and does not imply recommendation or endorsement by the U.S. Department of Agriculture.

^{*} Corresponding author. Fax: +1 301 504 5992.

E-mail address: baronej@ba.ars.usda.gov (J.R. Barone).

feathers and quill for several species of birds are in the range of 3–10 GPa and 100–200 MPa, respectively, depending on the portion of the feather measured and the moisture in the keratin.

Much less is known about the physical properties of the fiber portion of the feather. The quill is predominantly β -sheet protein structure and may differ in properties from the fiber [17]. Recently, George et al. [23] reported the mechanical properties for turkey feather fiber. However, the values are reported in units of denier so it is difficult to compare to units of length and stress without knowledge of the density of the fibers. In addition, turkey feather fiber is much larger in diameter than poultry feather fiber.

The major disadvantage to using organic fibers is that organic fibers begin to degrade at temperatures that are concurrent with processing temperatures typically experienced by commodity thermoplastic polymers. Therefore, novel processing techniques must be employed to retain the intrinsic properties of the organic fibers by processing at reduced temperatures. The high melting and degradation temperature of the poultry feather fiber makes it a good agricultural additive to be utilized in traditional polymers processed at high temperature.

Lundquist et al. [5] made composites from China reed fibers. These researchers proposed several different methods of spraying the fibers with polymer solutions to obtain a material that could be molded without an extruder compounding step. Other researchers utilize polymers such as thermosetting epoxies with flax fibers [24] or polyurethanes with sisal fibers [25] that can be molded at low temperature. These techniques carefully avoid processing at temperatures similar to the degradation temperature of the fibers. Dweib et al. [26,27] use a vacuum-assisted resin transfer molding process to mold feather fiber composites from epoxidized soybean oil. The composites are processed at low to moderate temperatures to avoid fiber degradation.

There are some studies detailing the incorporation of organic fibers in plasticized polymers. Oksman et al. [28] mixed flax fibers into plasticized polylactic acid (PLA) to obtain composites with increased mechanical properties over the plasticized PLA alone. At room temperature, PLA is in a glassy state and plasticizing lowers the glass transition temperature to below room temperature, giving plasticized PLA thermal and mechanical properties similar to polypropylene (PP). The composites are compounded on an extruder at temperatures of about 180 °C, which is a typical temperature for thermoplastic processing. Jana and Prieto [7] plasticized polyphenylene ether (PPE) to reduce the glass transition temperature. PPE is processed at around 260 °C, which is well above its glass transition of 212 °C. Plasticizing allows for processing at 200–220 °C with wood fibers so as to minimize fiber degradation. In the case of Oksman et al. and Jana and Prieto, the composite of plasticized

polymer and cellulose fiber has increased properties over the plasticized polymer alone. However, the modulus and tensile strength of the plasticized polymer/cellulose fiber composite are comparable to that of the virgin, unplasticized polymer. The advantage of plasticization then is to lower the processing temperature and to increase “toughness” as manifested in a larger elongation to break and increased impact properties.

Some studies utilize compression molding of fibers and polymer to eliminate the compounding step and perform mixing and molding in one step [13,29]. This minimizes length reduction of the fibers and the time the fibers spend at high temperature. These methods basically spread cellulose fibers evenly between polymer films and then press the “sandwich” in a compression molder at 180 °C for several minutes. Bullions et al. [30,31] prepare composites of kenaf bast, wood pulp, and poultry feather fiber by mixing the fibers with polypropylene fibers to form a slurry, then passing the slurry through a 182 °C oven at a fast rate to melt the PP fibers but not degrade the natural fibers and a prepreg is formed. The prepreg is then compression-molded into laminate plates at 4.4 MPa and 180 °C.

Colom et al. [6] prepare HDPE/wood fiber composites using a compounding step at 160 °C in a roll mill and a molding step at 150 °C in a compression molder for up to 20 min. This is a more traditional polymer composite processing method. Schuster [32] compounds feather fiber in polypropylene on an extruder at 200 °C.

In this paper, keratin feather fiber is incorporated into high-density polyethylene (HDPE) at a constant weight percentage of 20 wt%. The composites are mixed in a Brabender mixing head at set temperatures ranging from 140 to 200 °C, for times up to 30 min, and speeds from 50 to 100 rpm. Following mixing, tensile bars are prepared by compression molding at temperatures from 160 to 220 °C over time periods of 0–7 min. In each case, virgin HDPE is prepared in the same manner. All samples are tested in uniaxial tension to assess elastic modulus (E), peak stress (σ_p), and strain at peak stress (ϵ_p). Scanning electron micrographs of the fracture surfaces denote fiber condition and fiber/polymer interactions.

2. Experimental

2.1. Materials

2.1.1. Keratin feather fiber

Keratin feather fiber is obtained from Featherfiber® Corporation (Nixa, MO). The keratin feather fiber is cleaned and separated from the quill fraction according to a process developed and patented by the USDA [33]. The feather fiber is semi-crystalline and has an average diameter of $\approx 5 \mu\text{m}$. Feather fiber has an experimentally determined density of 0.89 g/cm^3 [15]. Hong and Wool

[34] report a density value for hollow keratin fiber of 0.80 g/cm^3 although the type of keratin fiber is not known. Fiber lengths of 0.1 and 0.0053 cm are made by grinding and sieving processes previously described [15]. Average fiber lengths are found by imaging the ground fiber in the scanning electron microscope (SEM). The average fiber length found in SEM correlates well with the predominant fraction obtained from sieving and the predominant fraction is the one used in the experiments.

2.1.2. Polymer–matrix

The matrix material is a HDPE commercially available from Exxon called HDPE 7760. The HDPE has a melt flow index (MFI) of 0.06 g/10 min at 190 °C and 2.16 kg and a density of 0.95 g/cm^3 in the solid-state. The melting temperature and percent crystallinity of HDPE 7760 are determined from differential scanning calorimetry according to ASTM D3417 and ASTM D3418 using a TA Instruments DSC 910S. The melting temperature is 133 °C and the percent crystallinity is 73% [35].

2.2. Composite preparation

2.2.1. Compounding step

The first set of experiments is to delineate the optimum compounding time at a given speed to achieve high fiber dispersion and still maintain fiber and polymer properties. Composites are compounded by first adding the HDPE into a Brabender mixing head with the mixer blades rotating at 50, 75, or 100 rpm. A low set compounding temperature, T_{set} , of 140 °C is chosen because it is above the melt temperature of HDPE 7760 and avoids any degradation of the fibers. Once the HDPE has melted inside the mixing head (≈ 1 min) the respective amount of keratin feather fiber is added. Feather fiber loading is kept constant at 20 wt% or $\phi_f = 20.97$ volume percent (vol%). It takes ≈ 2 min to load the feather fiber into the mixing head at 50 rpm, 1.5 min at 75 rpm, and 1 min at 100 rpm. So the total time to add the polymer and fiber into the mixing head is 3, 2.5, and 2 min at 50, 75, and 100 rpm, respectively. The mixing head is filled to 70% of its capacity by volume. The maximum melt temperature measured over the 15 min compound time, T_{actual} , is monitored independently. Compounds are mixed for 2–30 min. The mixing times represent the total mixing time, including the loading of material.

The second set of experiments involves finding the optimum compounding temperature. Compounding is performed at 50 rpm for a constant time of 15 min. Set temperature is varied from 140 to 200 °C. Table 1 lists the set temperature of the mixing head, T_{set} , and the actual steady-state melt temperature measured inside the mixing head, T_{actual} , over the compounding time.

Table 1

Compounding conditions for HDPE 7760 and HDPE 7760/20 wt% feather fiber composites at 50 rpm

T_{set} (°C)	Control T_{actual} (°C)	0.0053 cm T_{actual} (°C)	0.1 cm T_{actual} (°C)	Compound time (min)
140	167	167	173	10, 15, 20, 25, 30
160	187	190	194	15
180	205	208	207	15
200	223	226	226	15

After removal from the Brabender mixing head, three films of each material are prepared in a Carver Press Autofour/30 Model 4394 compression molder. The material is sandwiched between Teflon-coated aluminum foil and pressed at 5.9 MPa and 160 °C for 18 s. The film/foil sandwich is removed from the press and allowed to cool to room temperature before separating. Images of the films are obtained and analyzed using UTHSCSA Image Tool v. 3.0 [36]. The state of dispersion is assessed by measuring the total fiber agglomerate area at a given time, A_t , relative to the original fiber agglomerate size, $\phi_f A$, where A is the unit area of the film sampled for agglomerates. Kuroda and Scott [37] show that the compression-molding step has no effect on the state of dispersion.

2.2.2. Molding step

To mold samples for testing, the three thin sheets are cut into quarters, stacked on top of each other, sandwiched between Teflon-coated aluminum foil, and pressed in the compression molder at 160 °C and 0.9 MPa for 3 min. After pressing, the films are removed from the press and air cooled to room temperature. This results in triangular panels ≈ 0.3 cm in thickness and sides of 10 cm \times 10 cm \times 14 cm. Type IV dogbone samples for testing according to ASTM D638 are machined from the films.

To study the effect of high temperature molding, samples are molded at 200 °C from 2 to 7 min. A second set of samples is molded at 220 °C from 0.75 to 2.50 min. These samples are molded with 0.3 cm thick aluminum shims between the Teflon-coated sheets to prevent the composite melt from pressing out to very thin dimensions. The applied pressing force is 2.1 MPa. Following pressing, the samples are removed from the press and air cooled to room temperature. Type IV dogbone samples can then be machined from the molded composites.

2.3. Composite testing

Composite samples are allowed to sit at ambient conditions for one week before testing. Uniaxial tensile testing is performed using a Com-Ten Industries 95 RC Test System. The applied testing speeds are 2.5 cm/min (1 in./min) and 12.7 cm/min (5 in./min). A minimum of three samples of each composite is tested.

2.4. Scanning electron microscopy

The fracture surfaces are excised from the failed tensile bars using a scalpel blade and transferred onto an aluminum SEM stub. The sample is then sputter coated with platinum. A JEOL 6400 scanning electron microscope (SEM) is used at an electron beam accelerating voltage of 2 kV.

3. Results and discussion

3.1. Composite compounding

3.1.1. Dispersion kinetics of fibers in HDPE

The degree of fiber dispersion is monitored by mixing 20 wt% 0.1 cm long fiber composites from 0 to 30 min. All samples are mixed at a set temperature of $T_{\text{set}} = 140^\circ\text{C}$. Fig. 1 shows the agglomerate fraction, af , as a function of time at three compounding speeds, where $af = A_t/(\phi_f A)$. Also shown above each point is the measured T_{actual} . Viscous dissipation increases with compounding speed resulting in an increased melt temperature. It is observed from the dispersion kinetics that the time for complete dispersion, t_d , of $\phi_f = 20.97$ vol% of 0.1 cm keratin feather fiber in HDPE 7760 is 15 min at 50 rpm, 7 min at 75 rpm, and 6.5 min at 100 rpm. The maximum strain rate, $\dot{\gamma}_{\text{max}}$, in the mixing head can be calculated from the angular speed, ω , of the mixing blade: $\dot{\gamma}_{\text{max}} = (\pi D \omega)/H$, where H is the smallest gap between the mixing blade and the mixing bowl and D is the diameter of the mixing blade [38].

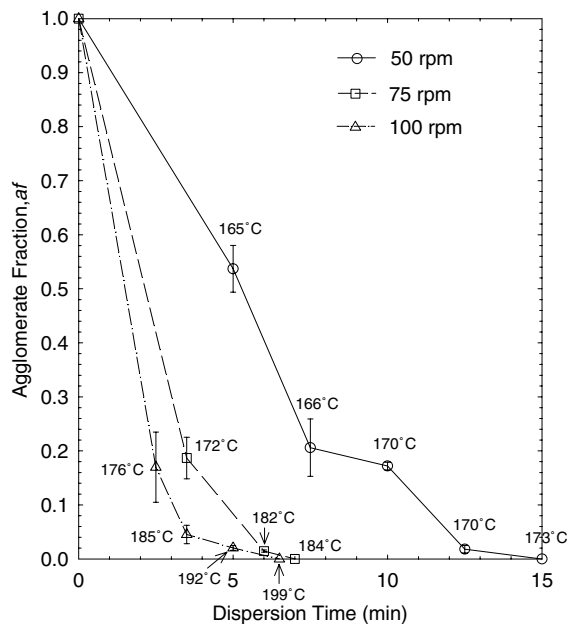


Fig. 1. Agglomerate fraction (af) vs. dispersion time at 50, 75, and 100 rpm with concurrent melt temperatures.

There is a large body of work on dispersion of fiber agglomerates in various fluids. The break-up of an agglomerate is described as a strain-induced process where the strain, γ , required is $\gamma = \dot{\gamma} t_d$ [39,40]. The maximum strain rate values at 50, 75, and 100 rpm are 68.25, 102.38, and 136.50 s^{-1} , respectively. This translates into total strain values for dispersion of 61,000, 43,000, and 53,000, respectively. So the total strain required to disperse all of the material is quite large. The smallest total strain is at 75 rpm, which suggests that this is the most efficient mixing speed of the three used. Closer inspection of Fig. 1 shows that the split between the 50 and 75 rpm curves is larger than the split between the 75 and 100 rpm curves. This is indicative of the non-linear viscoelastic nature of the HDPE/fiber composite melt.

3.1.2. Effect of compounding speed on composites

Fig. 2 shows the effect of compounding speed on composite tensile properties. All of the composites are prepared at $T_{\text{set}} = 140^\circ\text{C}$ for 15 min and tested at 2.5 cm/min. First, addition of fiber to the polymer increases modulus and decreases peak stress and strain at peak stress. Schuster [32] reports that there is no effect on tensile strength or modulus when 3.5 wt% of feather fiber is added to maleic anhydride modified polypropylene. However, Schuster observes a decrease in impact strength and ultimate elongation. Bullions et al. [31] also notice an increase in modulus with addition of feather fiber to polypropylene but a decrease in tensile strength. Only after addition of maleic anhydride polypropylene is there a small increase in tensile strength. Compound-

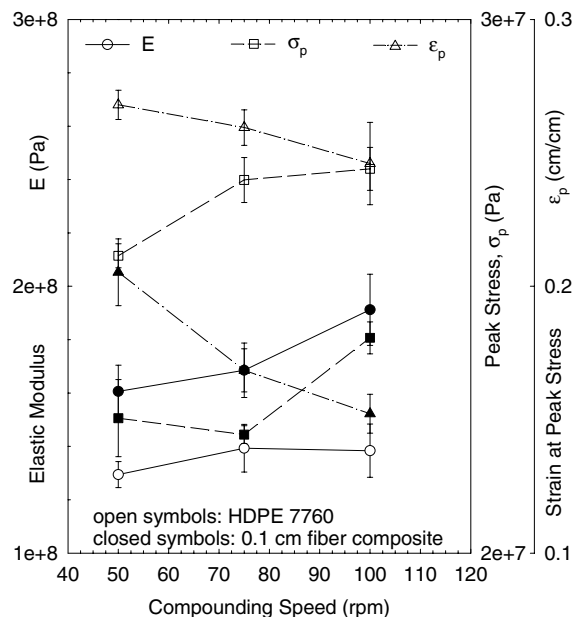


Fig. 2. Tensile properties of HDPE 7760 and 20 wt% 0.1 cm fiber composites after compounding at $T_{\text{set}} = 140^\circ\text{C}$ for 15 min at 50, 75, and 100 rpm and molded at 160°C for 3 min. Test speed is 2.5 cm/min.

ing speed appears to have an effect on the tensile properties of the composites. As compounding speed increases, so does the modulus and peak stress with a concurrent decrease of strain. The effect of compounding speed on tensile properties does not appear to be as pronounced in HDPE 7760. It has been shown that the weight average molecular weight (M_w) of polyethylene will increase during extrusion and is related to extrusion speed, temperature, and presence of oxygen [41]. The addition of fibers to the polymer increases the viscosity of the melt and thus the applied deformation at a given compounding speed compared to HDPE 7760. Shear heating effects are also more pronounced for the composites at $T_{set} = 140$ °C than for HDPE 7760 as shown in Table 1. The composite samples depicted in Fig. 2 have experienced higher deformations and temperatures over HDPE 7760 in the melt state. This effect is magnified as composite compounding speed increases. Therefore, an increase of M_w in the matrix portion of the composites would be consistent with the observed increased modulus and stress at higher compounding speeds for the composites.

The color and surface quality of each sample are also assessed. Table 2 contains information on the color (designated by a number) and surface quality (designated by a letter) of the samples as a function of compounding speed. The virgin HDPE 7760 samples are completely white in color but adding keratin feather fiber changes the color to off-white. The color of the composites resembles the color of other polyolefin-based composites such as glass fiber or calcium carbonate reinforced polyethylene. The same rating system is used for all of the comparisons of surface quality and color in the tables. A temperature increase resulting from increased viscous dissipation at higher compounding speeds discolors the composites.

SEM imaging of the fracture surfaces reveals the presence of loose or “pulled-out” fibers as shown in Fig. 3(a) at 200×. SEM shows no discernible decrease in length of the pulled-out fibers as compounding speed is increased. The pictured sample is compounded at 140 °C for 15 min at 50 rpm and molded at 160 °C. Zooming in on the fibers shows that there are voids in the polymer matrix

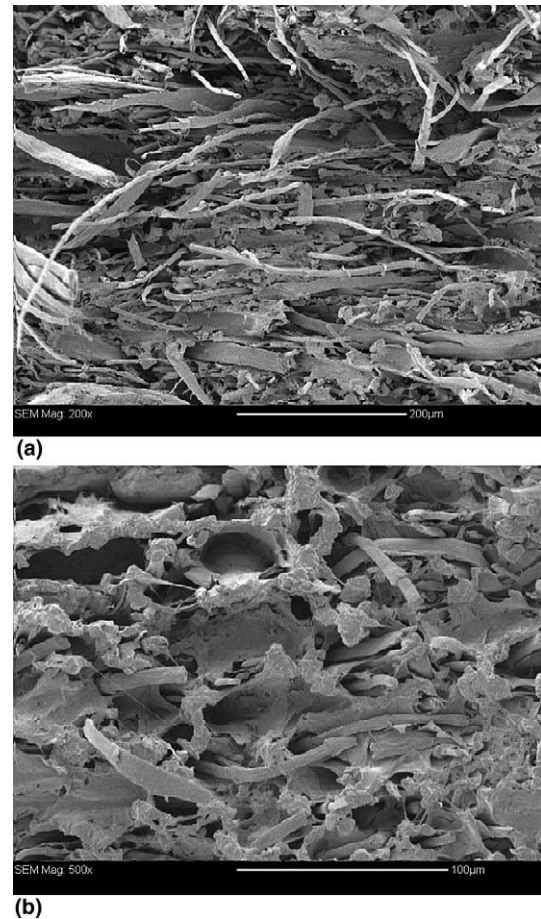


Fig. 3. SEM micrographs of HD7760/20 wt% 0.1 cm keratin feather fiber composite fracture surfaces compounded at $T_{set} = 140$ °C, 50 rpm, 15 min at (a) 200× and (b) 500× magnification.

around the fibers as shown in Fig. 3(b) as well as voids in the polymer–matrix where fibers once resided. There is little adherence of the polymer to the fibers. This is consistent with the observed decrease of peak stress with the addition of fiber as observed in Fig. 2. Bullions et al. show similar results for PP/feather fiber composites but are able to increase polymer/fiber adhesion through the use of maleic anhydride modified PP.

3.1.3. Effect of compounding time on composites

Fig. 4 shows the effect of compounding time on the tensile properties of HDPE 7760/20 wt% 0.1 cm keratin feather fiber composites prepared at $T_{set} = 140$ °C and 50 rpm and tested at 2.5 cm/min. Color and surface quality of the composites do not change as a function of compounding time. The mean modulus values of the composites are higher than the base polymer, but the mean values do not lie significantly outside of the standard deviation as represented by the error bars. The composite mixed for 10 min does not have a high modulus maybe because of a lack of fiber dispersion. The σ_p results do not show a lack of dispersion, but

Table 2
Sample quality as a function of compounding speed at $T_{set} = 140$ °C for 15 min

Speed (min)	HDPE 7760	T_{actual} (°C)	20 wt% 0.1 cm Composite	T_{actual} (°C)
50	1,S	167	2,S	173
75	1,S	179	2.25,S	186
100	1.25,S	193	3.25,S	202

Color: 1, white; 2, off-white; 3, yellow; 4, dark yellow; 5, brown.

Surface quality: S, smooth; A, hard agglomerates formed and protruding from surface; R, rough, pitted surface and bubbles, voids inside.

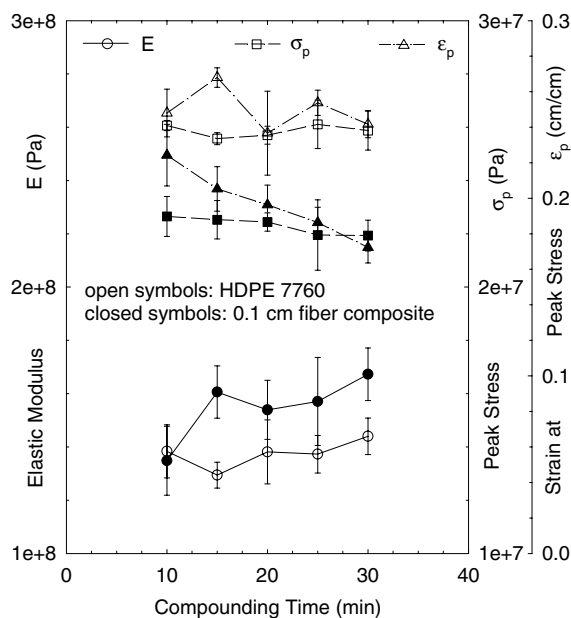


Fig. 4. Tensile properties vs. compounding time for HDPE 7760 and composites compounded at $T_{\text{set}} = 140^\circ\text{C}$ and 50 rpm and molded at 160°C for 3 min. Test speed is 2.5 cm/min.

the σ_p results are already affected by a lack of fiber/polymer interaction. After complete fiber dispersion, compounding time does not appear to have a marked effect on the E or σ_p results for the polymer or composite up to 30 min at low temperatures. However, the ϵ_p behavior of the composites decreases with compounding time, which may indicate some embrittlement. Again, the polymer and fiber do not interact very well as evidenced by the lower peak stress in the composite over the polymer and SEM observations. SEM analysis does not show any fiber length dependence on compounding time.

3.1.4. Effect of compounding temperature on composites

Fig. 5 shows the properties as a function of the actual melt temperature, T_{actual} , during compounding for the HDPE 7760 and HDPE 7760/20 wt% keratin feather fiber composites. All samples are compounded for 15 min. The mean moduli of the composites are higher than the virgin HDPE and lie outside of the standard deviation. Interestingly, compounding temperatures, T_{actual} , of 205, 207, and 208°C ($T_{\text{set}} = 180^\circ\text{C}$) give a maximum of elastic modulus for all of the samples. In the case of HDPE 7760, this may mean that there is a change in the molecular structure of the PE as already indicated. Table 3 compares the color and surface quality of the samples as a function of compounding temperature at constant compounding time and speed of 15 min and 50 rpm. It is observed that temperature has a marked effect on the color and surface condition of the composite tensile samples, especially at $T_{\text{actual}} = 226^\circ\text{C}$. The discoloration of the $T_{\text{actual}} = 207$ and 208°C

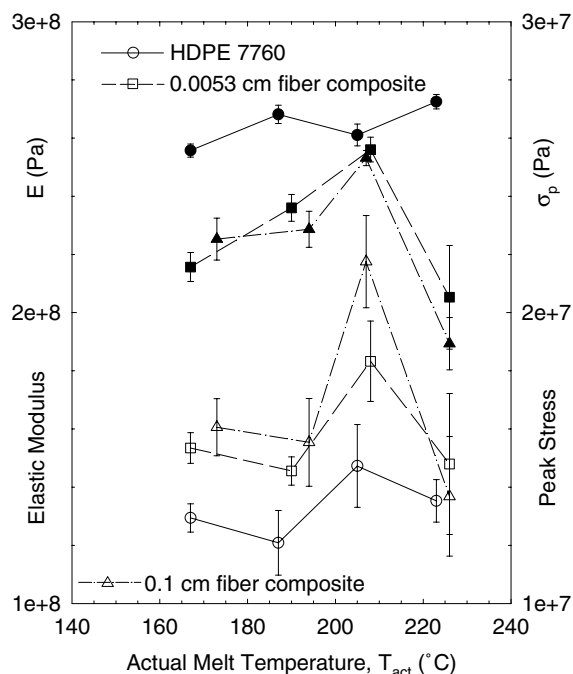


Fig. 5. Tensile properties vs. actual melt temperature during compounding for HDPE 7760 and composites compounded at 50 rpm for 15 min and molded at 160°C for 3 min. Open symbols are E and closed symbols are σ_p . Test speed is 2.5 cm/min.

Table 3

Sample quality as a function of compounding temperature at 50 rpm for 15 min; T_{actual} is in Table 1

T_{set} ($^\circ\text{C}$)	HDPE 7760	20 wt% 0.0053 cm Composite	20 wt% 0.1 cm Composite
140	1,S	2,S	2,S
160	1,S	3,S	3,S
180	1.5,S	4,S	4,S
200	1.5,S	5,A	5,A

Color: 1, white; 2, off-white; 3, yellow; 4, dark yellow; 5, brown.

Surface quality: S, smooth; A, hard agglomerates formed and protruding from surface; R, rough, pitted surface and bubbles, voids inside.

composites occurs after about 6 min of mixing. Above 210°C , the modulus of the polymer and composites draws closer together probably because of fiber degradation. Discoloration of the composite during compounding at $T_{\text{actual}} = 226^\circ\text{C}$ begins after about a minute. In Fig. 6(a), SEM analysis shows that there are lots of particles, but no intact fibers after processing at 226°C . So the loss of properties correlates with the severe degradation of the fibers. The mean modulus values of the 0.1 cm fiber composites ($L/D = 200$, $T_{\text{actual}} = 207^\circ\text{C}$) are higher than the values of the 0.0053 cm fiber composites ($L/D = 10$, $T_{\text{actual}} = 208^\circ\text{C}$) and lie outside of standard deviation. However, there does not seem to be a dependence of composite thermal stability on the length of the fiber used.

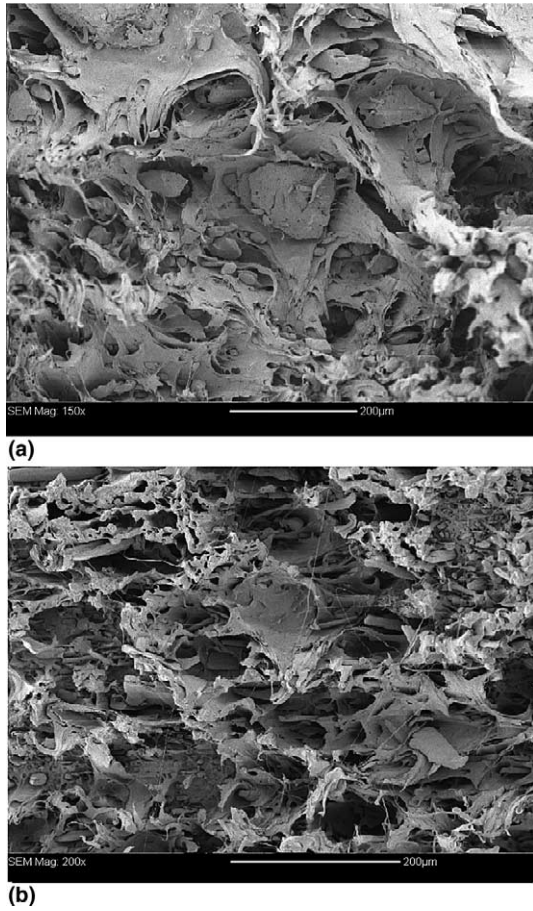


Fig. 6. SEM micrographs of HDPE 7760/20 wt% 0.1 cm composite fracture surfaces molded at 160 °C for 3 min and compounded at 50 rpm, 15 min and (a) $T_{\text{set}} = 200$ °C at 150 \times ; (b) $T_{\text{set}} = 180$ °C at 200 \times .

The peak stresses of the composites are again lower than that of the virgin polymer. The yield behavior of the composites appears to mimic the modulus behavior in the sense that the maximum peak stress values are obtained at $T_{\text{actual}} = 207$ and 208 °C. In fact, these composites have peak stress values comparable to HDPE 7760, which would indicate increased fiber/polymer interactions. In Fig. 6(b), SEM analysis shows that there are still some fibers embedded in the matrix although close inspection of the fibers indicates that there is some loss of surface roughness indicative of thermal degradation. Compared to Fig. 3(a), there are increased interactions at the higher temperature demonstrated by more loose fibers at the fracture surface of the lower processing temperature composite. Also, the matrix appears more deformed at $T_{\text{actual}} = 207$ °C than it does at $T_{\text{actual}} = 173$ °C. So, at compounding temperatures of 207 °C, the fiber/polymer interactions in the melt state are maximized relative to the other processing conditions used in this study. The increase in modulus at $T_{\text{actual}} = 207$ °C appears to be higher than that which can be attributed to an increase in polymer properties alone.

3.2. Composite molding

In polymer processing, compounding represents the first step. The second step is usually a molding operation at temperatures concurrent with the compounding temperature. Molding conditions comparable to those found in industry are chosen for the molding study. The effects of molding the HDPE/keratin feather fiber composites at temperatures of 200 °C or higher are studied not only because of applied relevance but because this region seems to be where the composites are least stable.

All of the samples evaluated for molding parameters are compounded at $T_{\text{set}} = 140$ °C, 50 rpm, for 15 min. The color and surface quality of the samples as a function of molding temperature and time at constant compounding conditions are given in Table 4. Fig. 7 shows that the modulus of HDPE 7760 seems to increase when molding at 220 °C for increasing time. Eventually, the curve for HDPE 7760 at 220 °C approaches the 200 °C molding results. For comparison, results for HDPE 7760 compounded in the same manner but molded at 160 °C for 3 min are presented. The 160 °C data is obtained at a test speed of 2.54 cm/min, but the dependency of properties on test speed was found to be weak for feather fiber/PE composites [15]. After about 2 min of molding, the modulus values for all of the HDPE 7760 samples, no matter what the molding temperature, are relatively similar. The E results for molding at 220 °C show a similar dependence on molding time. However, no samples were molded at 220 °C above 2.5 min because of severe sample degradation, so it is difficult to say if E would stabilize at longer times but given the amount of sample degradation, probably not. Molding involves the compression molding of several layers of material at 2.1 MPa. So, the minimum time required to get good bonding between layers could be 2 min at 2.1 MPa when molding well above the melting temperature of HDPE 7760.

Table 4
Sample quality as a function of molding temperature and time

T (°C)	Time (min)	HDPE 7760	20 wt% 0.1 cm Composite
200	2	1,S	2,S
	3	1,S	2,S
	5	1,S	3,S
	7	1,S	4,R
220	0.75	1,S	2,S
	1.5	1,S	3,R
	2.5	1,S	4,R

Color: 1, white; 2, off-white; 3, yellow; 4, dark yellow; 5, brown.

Surface quality: S, smooth; A, hard agglomerates formed and protruding from surface; R, rough, pitted surface and bubbles, voids inside.

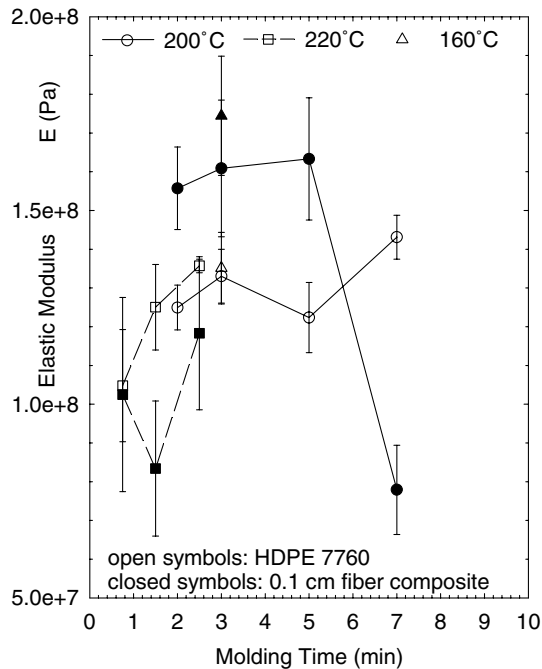


Fig. 7. Elastic modulus vs. molding time for HDPE 7760 and composites after compounding at $T_{\text{set}} = 140$ °C and 50 rpm for 15 min. Molding temperatures are 160, 200, and 220 °C. Test speed is 12.7 cm/min.

Fig. 7 also shows that the composite modulus will remain higher than the polymer modulus when molding for short times at 200 °C. However, longer molding times, i.e., greater than 6 min, cause too much fiber degradation and sample deterioration and the modulus decreases. Severe discoloration is observed after about a minute of molding which is similar to the observed discoloration after a minute of compounding at about 220 °C. Bullions et al. [31] observe color changes in samples at temperatures greater than 195 °C and Schuster [32] observes surface oxidation of the samples at 200 °C. Molding at 200 °C for 3 min produces a stable composite with properties similar to a composite molded at 160 °C for 3 min. This seems reasonable given the fact that discoloration, indicative of fiber degradation, is not observed at 200 °C until after 6 min of compounding or molding.

Figs. 8 and 9 show the peak stress and strain behavior, respectively, as a function of molding conditions. Again, the peak stress of the composites is lower than the virgin polymer so molding does not improve this behavior. Yield behavior does not change appreciably as a function of molding conditions for HDPE 7760. However, the composites fail at lower stresses than the base polymer and show a decreased strain at peak stress. The sample compounded at 200 °C for 7 min fails prematurely because it contains many voids and a pitted surface originating from fiber degradation. The yielding behavior of the composites is more sensitive to thermal

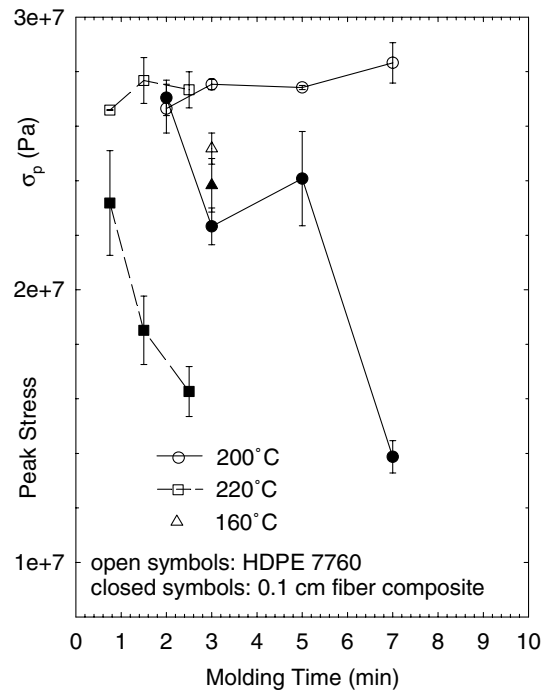


Fig. 8. Peak stress vs. molding time for HDPE 7760 and 20 wt% 0.1 cm composites after compounding at $T_{\text{set}} = 140$ °C and 50 rpm for 15 min. Molding temperatures are 160, 200, and 220 °C. Test speed is 12.7 cm/min.

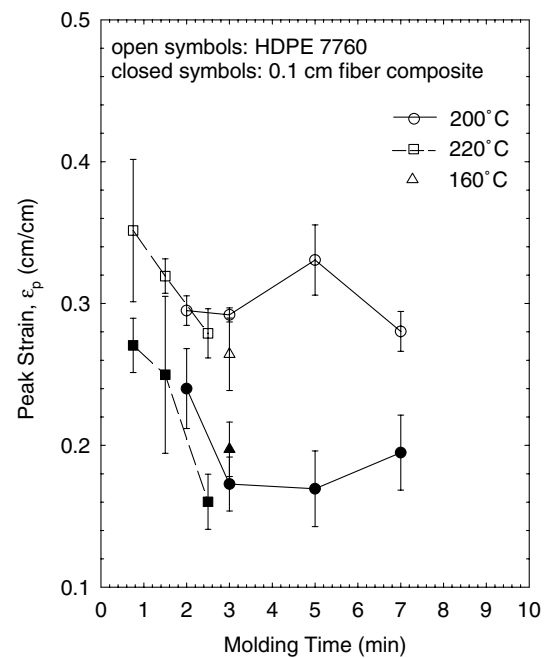


Fig. 9. Peak strain vs. molding time for HDPE 7760 and 20 wt% 0.1 cm composites after compounding at $T_{\text{set}} = 140$ °C and 50 rpm for 15 min. Molding temperatures are 160, 200, and 220 °C. Test speed is 12.7 cm/min.

degradation than modulus because the surface quality of the tensile bars is compromised. Once past the linear portion of the stress–strain curve, the samples yield pre-

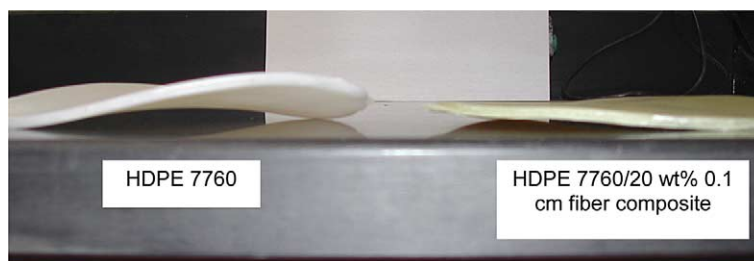


Fig. 10. HDPE 7760 panel (left) and HDPE 7760/20 wt% 0.1 cm fiber composite (right) compounded, molded, and cooled under the same conditions.

maturely because of surface defects originating from thermal degradation. This is the cause of the steady decrease of the yield point for the composites with increased molding time at 200 or 220 °C. At these temperatures, there is increased sample discoloration, sample surface roughness increases, and the presence of a distinct odor. As the keratin thermally degrades, it gives off more and more sulfur, bound water, and possibly other by-products that affect the polymer and composite overall.

Fig. 10 shows a HDPE 7760 panel on the left and a HDPE 7760/20 wt% 0.1 cm feather fiber composite panel on the right. Both panels were compounded at $T_{\text{set}} = 140$ °C for 15 min and 50 rpm then molded at 160 °C and 0.9 MPa for 3 min. The panels were both removed from the press and air-cooled to room temperature. It can be seen that the feather fiber composite experiences much less warpage after molding. This is advantageous because for some applications, the purpose of using additives is to simply maintain the dimensional stability of the molded part. Feather fiber provides dimensional stability during molding so fast molding cycle times can be used.

4. Conclusions

In this paper, conditions are described for the efficient compounding and molding of a keratin feather fiber/HDPE composite. The compounding study indicates that the best compounding conditions for producing keratin feather fiber/HDPE composites would be a compounding temperature of about 205 °C at 75 rpm in a Brabender mixing head. Optimum compounding conditions would maximize fiber/polymer interactions, minimize fiber degradation, and minimize viscosity in the melt state. Some embrittlement of the composite may occur at long compounding times, i.e., greater than 10 min, especially as temperature is increased.

When molding compounds at 2.1 MPa, the stiffness of the composites remains stable at 205 °C up to 6 min. However, after 6 min of molding the stiffness decreases and the sample color begins to darken. Sample

quality deteriorates after about 2 min of molding time at 200 °C or greater resulting in a low yield point. Typical injection molding applications take a fraction of this time for small to reasonably sized parts, i.e., tens of seconds, so it would be possible to effectively mold components at typical times and temperatures for polyolefins without significant material degradation.

Processing conditions are important so the intrinsic properties of the biologically derived fiber can be maintained. It is possible that keratin feather fiber has higher properties than polyolefins so reinforced composites can be obtained [19–22,31]. Keratin feather fiber has a lower density than polyolefins, which would result in composites of lower density [15,31,34]. In the present study, the density of the 20 wt% composite, assuming no voids, would be 0.94 g/cm³, which is lower than the density of HDPE 7760. It is found that processing of the natural fiber composite material can proceed at times and temperatures encountered during processing of polyolefins. This may make the feather fiber a good candidate for the modification of the tensile properties of polyolefins if suitable composite formulations and processing avenues can be found.

Acknowledgements

The authors thank Dr. Stephen Banovic of NIST for the SEM experiments on the composites.

References

- [1] Mohanty AK, Misra M, Drzal LT. Sustainable bio-composites from renewable resources: opportunities and challenges in the green materials world. *J Pol Env* 2002;10:19–26.
- [2] Bledzki AK, Gassan J. Composites reinforced with cellulose based fibres. *Prog Pol Sci* 1999;24:221–74.
- [3] Kalaprasad G, Mathew G, Pavithran C, Thomas S. Melt rheological behavior of intimately mixed short sisal-glass hybrid fiber-reinforced low-density polyethylene composites. I. Untreated fibers. *J Appl Pol Sci* 2003;89:432–42.
- [4] Ali R, Iannace S, Nicolais L. Effect of processing conditions on mechanical and viscoelastic properties of biocomposites. *J Appl Pol Sci* 2003;88:1637–42.

- [5] Lundquist L, Marque B, Hagstrand P-O, Leterrier Y, Manson J-AE. Novel pulp fibre reinforced thermoplastic composites. *Comp Sci Tech* 2003;63:137–52.
- [6] Colom X, Carrasco F, Pages P, Canavate J. Effects of different treatments on the interface of HDPE/lignocellulosic fiber composites. *Comp Sci Tech* 2003;63:161–9.
- [7] Jana SC, Prieto A. On the development of natural fiber composites of high-temperature thermoplastic polymers. *J Appl Pol Sci* 2002;86:2159–67.
- [8] Nunez AJ, Kenny JM, Reboredo MM, Aranguren MI, Marcovich NE. Thermal and dynamic mechanical characterization of polypropylene–woodflour composites. *Pol Eng Sci* 2002;42:733–42.
- [9] Oksman K, Clemons C. Mechanical properties and morphology of impact modified polypropylene–wood flour composites. *J Appl Pol Sci* 1998;67:1503–13.
- [10] Schneider JP, Myers GE, Clemons CM, English BW. Biofibers as reinforcing fillers in thermoplastic composites. *J Vinyl Add Tech* 1995;1:103–8.
- [11] Maldas D, Kokta BV. Composite molded products based on recycled polypropylene and woodflour. *J Therm Comp Mat* 1995;8:420–34.
- [12] Hughes M, Hill CAS, Hague JRB. The fracture toughness of bast fibre reinforced polyester composites. Part 1. Evaluation and analysis. *J Mater Sci* 2002;37:4669–76.
- [13] Jayaraman K. Manufacturing sisal–polypropylene composites with minimum fibre degradation. *Comp Sci Tech* 2003;63:367–74.
- [14] Rana AK, Mandal A, Bandyopadhyay S. Short jute fiber reinforced polypropylene composites: effect of compatibiliser, impact modifier, and fiber loading. *Comp Sci Tech* 2003;63:801–6.
- [15] Barone JR, Schmidt WF. Polyethylene reinforced with keratin fibers obtained from chicken feathers. *Comp Sci Tech* 2005;65:173–181.
- [16] Parkinson G. Chementator: a higher use for lowly chicken feathers? *Chem Eng* 1998;105(3):21.
- [17] Schmidt WF, Jayasundera S. Microcrystalline keratin fiber. In: Wallenberger F, Weston N, editors. *Natural fibers plastics, and composites-recent advances*. Dordrecht: Kluwer Academic Publishers; 2003. p. 51–66.
- [18] Schmidt WF, Line MJ. Physical and chemical structures of poultry feather fiber fractions in fiber process development. In: *TAPPI proceedings: 1996 nonwovens conference*. p. 135–40.
- [19] Fraser RDB, MacRae TP. Molecular structure and mechanical properties of keratins. *Symposia of the society for experimental biology number XXXIV: the mechanical properties of biological materials*. Cambridge: Cambridge University Press; 1980. p. 211–46.
- [20] Purslow PP, Vincent JFV. Mechanical properties of primary feathers from the pigeon. *J Exp Biol* 1978;72:251–60.
- [21] Bonser RC, Purslow PP. The Young's modulus of feather keratin. *J Exp Biol* 1995;198:1029–33.
- [22] Cameron GJ, Wess TJ, Bonser RHC. Young's modulus varies with differential orientation of keratin in feathers. *J Struct Biol* 2003;143:118–23.
- [23] George BR, Evazynajad A, Bockarie A, McBride H, Bunik T, Scutti A. Keratin fiber nonwovens for erosion control. In: Wallenberger N, Weston N, editors. *Natural fibers plastics, and composites-recent advances*. Dordrecht: Kluwer Academic Publishers; 2003. p. 67–81.
- [24] Van de Weyenberg I, Ivens J, De Coster A, Kino B, Baetens E, Verpoest I. Influence of processing and chemical treatment of flax fibres on their composites. *Comp Sci Tech* 2003;63:1241–6.
- [25] Tavares MIB, Mothe CG, Araujo CR. Solid-state nuclear magnetic resonance study of polyurethane/natural fibers composites. *J Appl Pol Sci* 2002;85:1465–8.
- [26] Dweib MA, Hu B, O'Donnell A, Shenton HW, Wool RP. All natural composite sandwich beams for structural applications. *Comp Struct* 2004;63:147–57.
- [27] Dweib M, O'Donnell A, Wool R, Hu B, Shenton T. Bio-based composite sandwich structures for construction applications. *CCM/UD Res Rev* 2003. Available from: http://www.ccm.udel.edu/reports-pubs/Spring03_reviews/Apr30/dweib.pdf.
- [28] Oksman K, Skrifvars M, Selin J-F. Natural fibers as reinforcement in polylactic acid (PLA) composites. *Comp Sci Tech* 2003;63:1317–24.
- [29] Wambua P, Ivens J, Verpoest I. Natural fibres: can they replace glass in fibre reinforced plastics. *Comp Sci Tech* 2003;63:1259–64.
- [30] Bullions TA, Hoffman D, Price-O'Brien J, Loos AC. Feather fiber/cellulose fiber/polypropylene composites manufactured via the wetlay papermaking process. In: *INTC2003 proceedings*.
- [31] Bullions TA, Gillespie RA, Price-O'Brien J, Loos AC. The effect of maleic anhydride modified polypropylene on the mechanical properties of feather fiber, kraft pulp, polypropylene composites. *J Appl Pol Sci* 2004;92:3771–83.
- [32] Schuster J. Polypropylene reinforced with chicken feathers. In: *14th International conference on composite materials*, San Diego, CA, July 14–18; 2003.
- [33] Gassner G, Schmidt W, Line MJ, Thomas C, Water RM. Fiber and fiber products from feathers. *United States Patent No.* 5,705,030; 1998.
- [34] Hong CK, Wool RP. Low dielectric constant materials from soybean oils and hollow keratin fibers. *CCM/UD Res Rev* 2003. Available from: http://www.ccm.udel.edu/reports-pubs/Spring03_reviews/Apr30/Hong.pdf.
- [35] Wunderlich B. *Thermal analysis*. New York: Academic Press; 1990. p. 280–92.
- [36] UTHSCSA Image Tool v. 3.0. Available from: <http://ddsdx.uthscsa.edu/dig/itdesc.html>.
- [37] Kuroda MMH, Scott CE. Initial dispersion mechanisms of chopped glass fibers in polystyrene. *Pol Comp* 2002;23:395–405.
- [38] Tadmor Z, Gogos CG. *Principles of polymer processing*. New York: Wiley; 1979. p. 449–52.
- [39] Pandya JD, Spielman LA. Floc breakage in agitated suspensions: theory and data processing strategy. *J Coll Int Sci* 1982;90:517–31.
- [40] Berzin F, Vergnes B, Lafleur PG, Grmela M. A theoretical approach to solid filler dispersion in a twin-screw extruder. *Pol Eng Sci* 2002;42:473–81.
- [41] Epacher E, Tolveth J, Stoll K, Pukanszky B. Two-step degradation of high-density polyethylene during multiple extrusion. *J Appl Pol Sci* 1999;74:1596–605.